

A review of selected issues concerning the chemistry in Venus' middle atmosphere

Franklin P. Mills^{a,*}, Mark Allen^{b,2}

^aResearch School of Physical Sciences and Engineering, Australian National University, Canberra 0200, Australia

^bJet Propulsion Laboratory, California Institute of Technology, Pasadena, CA 91109, USA

Accepted 10 April 2006

Available online 2 February 2007

Abstract

Even after decades of study using advanced observing instruments and sophisticated numerical models, a number of significant questions remain unanswered concerning the composition and chemistry of Venus' atmosphere. The primary chemical cycles and the interactions among sulfur and chlorine radicals in Venus' middle atmosphere are reviewed to assess the current status of our knowledge, identify unresolved questions, and assess how the Venus Express mission may contribute to their resolution.

© 2007 Elsevier Ltd. All rights reserved.

PACS: 92.60.H–; 96.30.Ea; 96.12.Jt

Keywords: Venus; Atmosphere; Chemical composition

1. Introduction

Prior investigations of Venus' atmospheric chemistry have deduced three primary cycles: the CO₂ cycle, the sulfur oxidation cycle, and the polysulfur cycle. Clear observational evidence supports the existence of the first two cycles, but many details of how these cycles operate in Venus' atmosphere remain unresolved. The observational evidence for the third cycle still is controversial and less is known about it.

Krasnopolsky and Parshev (1983), von Zahn et al. (1983), Krasnopolsky (1986), and Esposito et al. (1997) provide detailed reviews of our understanding of Venus' atmospheric chemistry in the early 1980's, mid-1980s, and mid-1990s, respectively. Krasnopolsky (2006a) and Mills et al. (2007) update those reviews by focusing on observations made over the past decade. This review complements these contemporary works by emphasizing

the synthesis of recent laboratory experiments and observations into atmospheric chemistry models and by connecting the expected contributions from Venus Express observations to gaps in our understanding of Venus' atmospheric chemistry.

Venus Express data have the potential to address several of the unresolved issues that remain. This review uses a one-dimensional photochemical model, described in Section 2, to illustrate some of the discussion points. Model and data shortcomings specific to each of the three primary chemical cycles are discussed in Sections 3–5. The possible contributions of coupled sulfur and chlorine chemistry are explored in some detail in Section 6. Prospects for developing an improved understanding of Venus' atmospheric chemistry based on data from Venus Express are summarized in Section 7.

2. Model description

The Venus model used here is based on the Caltech/JPL code (Allen et al., 1981) and solves the continuity equation simultaneously for 47 species. This model is similar to that used to study the photochemistry of Mars (Nair et al., 1994). It is a one-dimensional model which is converged to

*Corresponding author.

E-mail address: Frank.Mills@anu.edu.au (F.P. Mills).

¹Also at Fenner School of Environment and Society and Planetary Sciences Institute, Australian National University.

²Also at Division of Geological and Planetary Sciences, California Institute of Technology, Pasadena, CA 91125, USA.

a steady-state solution via a finite-difference iterative algorithm. The model atmosphere, noon local solar time (Seiff, 1983), extends from 58 to 112 km altitude with 2-km thick layers. The model represents the “global average” photochemistry, so diurnal variations have not been explicitly modeled. Photodissociation was calculated for 45° latitude at local noon and then divided by 2. The solar fluxes used represent high solar irradiance conditions. Diffuse radiation was calculated using the Feautrier method generalized to arbitrary anisotropic scattering with aerosol scattering properties based on Pioneer Venus measurements (Crisp, 1986). Photoabsorption and chemical kinetic data were drawn from critically reviewed compilations (e.g., DeMore et al., 1997) whenever possible. Changes in kinetic rate recommendations since 1997 are not expected to be significant. The nominal equilibrium constant for ClCO formation and decomposition, $K_{\text{ClCO}} = 1.6 \times 10^{-25} \exp(4000/T)$ (Sander et al., 2002) is based on laboratory work by Nicovich et al. (1990). Temperature dependent cross sections were used for CO₂ (Lewis and Carver, 1983; Shemansky, 1972), SO₂ (Freeman et al., 1984b; Hearn and Joens, 1991; Leroy et al., 1983; Manatt and Lane, 1993; Martinez and Joens, 1992; McGee and Burris, 1987; Sprague and Joens, 1995; Suto et al., 1982), O₃ (Anderson and Mauersberger, 1992; Burkholder and Talukdar, 1994; Freeman et al., 1984a; Griggs, 1968; Molina and Molina, 1986; Tanaka et al., 1953; Yoshino et al., 1988, 1993), and OCS (Molina et al., 1981). UV cross sections for photolysis of ClC(O)OO were included (Pernice et al., 2004). No reactive nitrogen species were included in the calculations. Vertical transport via eddy diffusion was set based on observations (Lane and Opstbaum, 1983; von Zahn et al., 1980; Woo and Ishimaru, 1981). The H₂O profile was fixed to match the equilibrium vapor pressure over 75 wt% sulfuric acid (Mills, 1999b). At the lower boundary, the mixing ratio for CO₂ was set to 0.965 (von Zahn et al., 1983), HCl to 0.4 ppm (Young, 1972; Connes et al., 1967), OCS to 1 ppb (as was assumed by Bezard et al., 1990), and SO₂ to 1 ppm. The concentration gradient at the lower boundary for all other species was set to zero. At the upper boundary, the upward flux of molecules, such as CO₂, was set equal to the downward flux of their photodissociation products to simulate photodissociation occurring above the upper boundary. Additional detail on the model and its inputs is available in prior publications (Mills, 1998, 1999a, b; Pernice et al., 2004; Mills et al., 2006).

3. CO₂ cycle

The CO₂ cycle, the dominant chemical cycle above Venus' clouds, involves the photodissociation of CO₂ on the day side, production of O₂, and conversion of CO and O₂ into CO₂. CO₂ and CO have been observed with mixing ratios of 0.965 (von Zahn et al., 1983) and $\sim 1 \times 10^{-5} - 3 \times 10^{-3}$ above ~ 60 km (Connes et al., 1968; Lellouch et al., 1994; Gurwell et al., 1995), respectively. Ground-

state O₂ has not been detected and the observational upper limits are equivalent to uniform mixing ratios above 60 km of 0.3–2 ppm (Traub and Carleton, 1974; Trauger and Lunine, 1983; Mills, 1999a). (A mixing ratio of 0.3 ppm corresponds to a column abundance of $1.5 \times 10^{18} \text{ cm}^{-2}$ above 58 km altitude.) An alternative and more restrictive interpretation of the smallest nondetection limit corresponds to an O₂ column abundance of $8 \times 10^{17} \text{ cm}^{-2}$ above 62 km (Krasnopolsky, 2006a). (The reported detection of O₂ with a mixing ratio of 44 ± 25 ppm near 52 km, Oyama et al., 1980 was marginal and has not been confirmed. Indirect tests suggest such a high abundance of O₂ near 52 km is not plausible (von Zahn et al., 1983; Krasnopolsky, 1986; Mills, 1999a).) The large observed abundance of CO₂, the low observed abundance of CO, and the stringent observational limit on ground-state O₂ imply production of CO₂ approximately balances its loss via photodissociation. In addition, rapid production of ground-state O₂ has been inferred from observations of intense airglow emission in the O₂(a¹Δ → X³Σ) band at 1.27 μm on both the day and night sides (Connes et al., 1979; Crisp et al., 1996). Numerical modeling, therefore, suggests CO₂ must be produced via catalytic processes because its direct production from CO, O, and O₂ is slow (Nair et al., 1994; Mills, 1998).

The identity of the chemical mechanism(s) by which CO₂ is produced in Venus' atmosphere, however, has not been resolved. The inability of previous photochemical models (Winick and Stewart, 1980; Krasnopolsky and Parshev, 1981a–c, 1983; Yung and DeMore, 1982) to match the current observational limit on the ground-state O₂ abundance was seen as their major failing. The calculated O₂ in these models exceeded the Trauger and Lunine (1983) observational limit by at least a factor of 2.5 (which is five standard deviations for the original interpretation of the observation). More recent modeling (Pernice et al., 2004; Mills et al., 2006; Sundaram et al., 2007) has identified two potential mechanisms by which CO could be oxidized at a sufficiently rapid rate in Venus' middle atmosphere (58–110 km) to reduce the calculated O₂ abundance to a level that is closer to the observational limit. One mechanism produces CO₂ via ClC(O)OO (Yung and DeMore, 1982), and is the basis for Schemes A, B, and C in the Appendix. This mechanism has been verified in laboratory experiments (Pernice et al., 2004), but none of the intermediate species have been observed yet. Detection of ClCO, ClC(O)OO, or COCl₂ would be a major confirmation of this mechanism. (COCl₂ is a likely by-product of these Schemes.) The second mechanism, Scheme D, oxidizes CO via (photocatalytic?) reactions on or within aerosols or cloud particles (Mills et al., 2006; Sundaram et al., 2007). The aerosol mechanism was postulated based on qualitative laboratory studies (Mills and Phillips, 1993, 1996; Rowland and Phillips, 2000; Rowland et al., 2002), and requires detailed laboratory confirmation. Atreya and Blamont (1990) suggested heterogeneous oxidation of CO might be important in Mars' atmosphere, but Choi and

Leu (1997) found the reaction probabilities for the heterogeneous oxidation of CO on inorganic oxides and on water ice were too small for this to be a significant source for CO₂. However, laboratory measurements of photocatalytic oxidation of CO on TiO₂ (Thevenet et al., 1974), which is more similar to the photocatalytic oxidation of CO on/in sulfuric acid proposed for Venus, suggest photocatalytic oxidation could be a significant source for CO₂ on Mars (Choi and Leu, 1997) and possibly on Venus.

Due to the difficulty that models have had in obtaining a calculated O₂ column abundance that is compatible with the observational limit, the primary issue in understanding the CO₂ cycle on Venus typically has been phrased in terms of reproducing this limit in model calculations. However, there are really four inter-related issues (and observational constraints) associated with modeling and understanding the CO₂ cycle. The first is the observational limit on ground-state O₂. The second is the intense oxygen airglow observed in the O₂(*a*¹Δ → X³Σ) and other bands. The third and fourth are the abundance ratio for CO/O₂ and the spatial distribution of CO (and presumably of O₂).

3.1. Ground-state O₂

The failure of spectroscopic searches to detect ground-state O₂ (Traub and Carleton, 1974; Trauger and Lunine, 1983; Mills, 1999a) can be expressed easily as a limit on absorption by O₂ but its translation into an upper limit on the column abundance has been subject to varying interpretation (Trauger and Lunine, 1983; Mills, 1999a; Krasnopolsky, 2006a). None of the instruments on Venus Express will be able to provide a detection of ground-state O₂ but Earth-based spectroscopy might.

3.2. Oxygen airglow

Huestis (2002), Slanger and Copeland (2003), and Slanger et al. (2006) provide excellent reviews of excited state oxygen chemistry and its application to Venus' atmosphere. The detailed processes associated with formation of O₂ from two oxygen atoms are very difficult to disentangle due to strong apparent interactions and inter-system crossings among the various excited states of O₂. One key conclusion from recent laboratory studies, however, is that a large fraction (possibly near 100%) of the O₂^{*} produced in Reaction 1 is likely to be produced in or to go through one of the Herzberg states of O₂ (*A*³Σ, *A*¹Δ, and *c*¹Σ) (Huestis, 2002), which are the upper source states for the three Herzberg bands.



A second key conclusion is that the interplay among the many vibrational levels of the three Herzberg states and the ⁵Π state is sufficiently strong that rapid population redistributions appear to occur within and among these four states so the net yield of O₂(*c*) from Reaction 1 on Venus may be near 100% (Slanger and Copeland, 2003).

Given the net yield of O₂(*c*) from Reaction 1 may be near 100%, the amount of O₂(*c*) that must emit a photon in the Herzberg II band to produce the observed airglow (Krasnopolsky et al., 1976; Lawrence et al., 1977; Krasnopolsky, 1983, 1986) is only 0.5% of the O₂(*c*) that is produced (Slanger et al., 2006). The remaining O₂(*c*) will be collisionally quenched to produce a broad range of vibrationally excited O₂ in the three lowest electronic states (*X*³Σ, *a*¹Δ, and *b*¹σ). Laboratory studies (Wildt et al., 1991; Knutsen et al., 1994; Bednarek et al., 1994; Wildt et al., 1988; Fink et al., 1991) as reviewed by Huestis (2002) suggest collisional quenching by CO₂ of O₂(*c*) and O₂(*b*) leads to O₂(*a*¹Δ) with net yields ~95%. Hence, the net yield of O₂(*a*¹Δ) from Reaction 1 may be ~95%. Smaller (more conservative) net yields of O₂(*a*¹Δ) from Reaction 1 were assumed in the photochemical model calculations presented in Table 1: 0.6 for *M* = N₂ and 0.75 for *M* = CO₂ (Crisp et al., 1996). Even with these conservative net yields and a ground-state O₂ column abundance that is an order of magnitude smaller than in the Yung and DeMore (1982) Model C, Table 1 shows that model calculations can produce “global average” 1.27 μm airglow intensities that are in reasonable agreement with the observed “global average.”

Venus Express airglow observations will provide a much more solid understanding of typical atmospheric conditions, particularly on the day side. A high degree of correlation between CO abundance and O₂ airglow intensity would confirm the role of dynamics in controlling the distribution of these species. An anti-correlation between oxygen green line emission and 1.27 μm airglow would lend support to the O₂(*c*) mechanism for CO oxidation, Scheme E, that was recently proposed (Slanger et al., 2006; Mills et al., 2006).

3.3. CO abundance and distribution

There are two issues with the existing state of comparisons between models and observations for CO. The first is that the current proposed mechanisms for oxidation of CO do not yield the large ratio of CO to O₂ that is observed. Table 1 and Fig. 1 illustrate how the reductions in the modeled O₂ abundance that result from enhancements in the production rate for CO₂ via the ClC(O)OO mechanism are accompanied by corresponding decreases in the modeled CO mixing ratio. Similar results are found using the aerosol mechanism (Sundaram et al., 2007). For the calculations in Table 1 and Fig. 1, the uncertainty in the equilibrium constant was calculated via (Sander et al., 2002),

$$f(T) = f(298 \text{ K}) \exp \left[\Delta B \left(\frac{1}{T} - \frac{1}{298} \right) \right], \quad (2)$$

where *f* = uncertainty, *T* = temperature, Δ*B* = uncertainty in the equilibrium constant's exponential factor which is 500 K for ClCO, and *f*(298) = 5 for ClCO. The rate coefficient for the thermal decomposition reaction for

Table 1
Comparison of model calculations and observations

Parameter	Observation	Model calculation			
		+2 σ^a	+1 σ	+0.5 σ	Nominal ^b
O ₂ column (10 ¹⁸ cm ⁻²)	<0.8 ^c , <1.5 ^d	2.0	2.4	3.1	8.6
O ₂ (<i>a</i> ¹ <i>A</i> → <i>X</i> ³ Σ) 1.27 μ m	1.5 (day) ^e	1.2 ^f	1.3 ^f	1.3 ^f	1.5 ^f
Airglow emission (MR) ^g	1–1.2 (night) ^h				
S ₈ production (10 ⁹ cm ⁻² s ⁻¹)		8.6	5.4	1.2	~0
H ₂ SO ₄ production (10 ¹¹ cm ⁻² s ⁻¹)	~2–10 ⁱ	4.0	4.2	4.6	4.8

^aCICO thermal stability increased by twice the assessed uncertainty in the equilibrium constant (Sander et al., 2002) and model atmosphere temperatures (Seiff, 1983) at 84–90 km were decreased by 6 K.

^bThe nominal CICO equilibrium constant was used, but the model atmosphere temperatures (Seiff, 1983) at 84–90 km were decreased by 6 K.

^cKrasnopolsky (2006a).

^dTrauger and Lunine (1983).

^eConnes et al. (1979).

^fGlobal (diurnal) averages.

^g1 mega-Rayleigh (MR) = 10¹² photons cm⁻² s⁻¹ into 4 π sr.

^hCrisp et al. (1996) and Connes et al. (1979).

ⁱYung and DeMore (1982) and Winick and Stewart (1980).

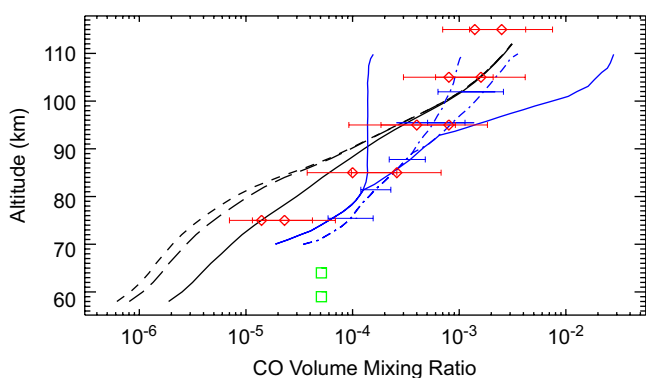


Fig. 1. Observed and modeled CO mixing ratios. Calculated profiles are global averages from the +2 σ (short-dashed black line), +1 σ (long-dashed black line), and nominal (solid black line) CICO thermal stability models. (See notes for Table 1.) The dash-dot blue lines are the CO mixing ratios deduced from millimeter-wave observations at 6 am and 12 am Venus Local Time (VLT) in 1990 (Clancy and Muhleman, 1991). The solid blue lines are the CO mixing ratios deduced from millimeter-wave observations at 3 am and 9 am VLT in 1986 (Clancy and Muhleman, 1991). The green squares indicate the revised (Young, 1972) day side CO mixing ratio derived from observations in 1966 (Connes et al., 1968). The two altitude locations mark the two likely altitude ranges for the observation based on the revised interpretation (Young, 1972). The red diamonds are the minimum and maximum CO mixing ratios observed on the night side in 1991 (Lellouch et al., 1994).

decomposes and thereby enhance the production rate for CO₂. The low CO abundances that accompany the low O₂ abundances in these model calculations may indicate this modeling approach either is not appropriate or is not complete. However, the observational record for CO is incomplete in spatial coverage, particularly on the day side, and observations on the night side indicate substantial temporal variability (Fig. 1). Three-dimensional maps of CO would markedly improve the quality of data against which photochemical model calculations can be compared. Vertical profiles of CO for 50–100 km altitude would enable photochemical models to assess the vertical profile of the rate of CO oxidation. Furthermore, temporal variations in the distribution of CO as observed by Venus Express, when combined with the long time base of ground-based observations, may provide the necessary context for understanding how the composition of the middle atmosphere on Venus may have changed over the past three decades (Esposito et al., 1988; Clancy and Muhleman, 1991; Lellouch et al., 1994; Na et al., 1994).

The second issue in the current state of comparisons between model calculations and observations for CO is the lack of coupling between chemical and dynamical effects in existing models. Models with simple dynamics and chemistry have been quite successful at explaining the CO distribution above ~90 km altitude (Lellouch et al., 1994; Gurwell et al., 1995), indicating that dynamical influences need to be considered in modeling the full CO₂ cycle. No model has been constructed to date that incorporates the full chemistry of the CO₂ cycle and transport of species due to dynamics; the observational data needed to develop and test a good chemical transport model (CTM) have not existed. Venus Express observations of winds and temperatures will provide the data required for creation of a CTM, and contemporaneous observations of CO should provide an excellent test of the CTM's capabilities.

CICO was decreased by 0.5, 1, and 2 times this uncertainty for the +0.5 σ , +1.0 σ , and +2.0 σ calculations, respectively, in Table 1 and Fig. 1. The nominal temperatures at 84–90 km were decreased by 6 K to further enhance the stability of CICO. This change in temperatures is well within the variability observed on the night side of Venus (Clancy et al., 2003). These increases in the thermal stability of CICO enhance the likelihood that CICO will react with O₂ to form CIC(O)OO before CICO thermally

4. Sulfur oxidation cycle

This cycle involves primarily the oxidation of SO₂ in the upper cloud to form H₂SO₄, condensation and downward transport of the sulfuric acid, and evaporation and decomposition in the lower atmosphere to produce SO₂, CO₂, and H₂O. Good observational evidence exists for most steps in this cycle (Krasnopolsky and Pollack, 1994), but there are inconsistencies among the models that have been used to study the various parts of the cycle (Esposito et al., 1997). Krasnopolsky and Pollack (1994) developed two models for the condensation and evaporation of sulfuric acid that gave good agreement with a range of observational constraints at 30–50 km altitude. A new analysis of Venera optical spectra (Ignatiev et al., 1997) agrees well with interpretations of Earth-based observations (Pollack et al., 1993) so that Model 1 from Krasnopolsky and Pollack (1994) is now strongly favored. The required production rate for H₂SO₄ in this model is $2.2 \times 10^{12} \text{ cm}^{-2} \text{ s}^{-1}$. Previous photochemical models predicted H₂SO₄ production rates of $9 \times 10^{11} - 1.1 \times 10^{13} \text{ cm}^{-2} \text{ s}^{-1}$ (Yung and DeMore, 1982; Krasnopolsky and Pollack, 1994), but the +2σ, +1σ, and +0.5σ models in Table 1, which have better agreement with the observational limit on O₂, have smaller H₂SO₄ production rates, $4 - 5 \times 10^{11} \text{ cm}^{-2} \text{ s}^{-1}$. In addition, Krasnopolsky (2006b), found that inclusion of NO_x in a photochemical model opened additional important pathways for oxidizing SO and producing O₂ via



So, Reactions (3) and (4) may further reduce the H₂SO₄ production rates in photochemical models. Previous observational estimates of the H₂SO₄ production rate were in the range of $2 \times 10^{11} - 1 \times 10^{12} \text{ cm}^{-2} \text{ s}^{-1}$ (Winick and Stewart, 1980; Yung and DeMore, 1982).

If the H₂SO₄ production rate in the upper cloud is as large as has been modeled by Krasnopolsky and Pollack (1994), then a critical process may be missing from photochemical models. Production of H₂SO₄ via ClSO₄ (DeMore et al., 1985) could be a very efficient mechanism for oxidizing SO₂ but has not been tested in more recent models, see Section 6.2.

5. Polysulfur cycle

The polysulfur cycle involves photodissociation of SO₂ or OCS, formation of polysulfur (S_x), downward transport of the S_x, and thermal decomposition followed by reaction with CO in the lower atmosphere to produce OCS or reaction with SO₃ to form SO₂. The polysulfur cycle was originally proposed when OCS was believed to be the primary sulfur species in Venus' atmosphere (Prinn, 1978). More recently, Krasnopolsky and Pollack (1994) established a relationship between the fluxes

of H₂SO₄, CO, and S,

$$\Phi_{\text{H}_2\text{SO}_4} = \Phi_{\text{SO}_3} = \Phi_{\text{CO}} + 2\Phi_{\text{S}} \quad (5)$$

for the situation where CO and SO₂ oxidation are comparable in importance. They found $\Phi_{\text{S}} = 2.5 \times 10^{11}$ or $\Phi_{\text{S}_8} = 3 \times 10^{10}$ in their Model 1 (Krasnopolsky and Pollack, 1994), which gave a mass ratio S_x/H₂SO₄ in Model 1 of 0.04. This is somewhat smaller than the nominal mass ratio, 0.1–0.15, inferred from Vega gas chromatograph measurements (Porshnev et al., 1987; Krasnopolsky, 2006a). S₃ has been reported in the lower atmosphere (Maiorov et al., 2005), but there is some controversy over this detection (von Zahn et al., 1983). There has been no definitive detection of S_x in the middle atmosphere, but the presence of S_x aerosol has been inferred from measurements by the Vega gas chromatograph (Porshnev et al., 1987). S_x has been suggested as a potential candidate for the UV absorber at 320–500 nm (Esposito et al., 1997; Krasnopolsky, 2006a). Photochemical models (Winick and Stewart, 1980; Yung and DeMore, 1982) have sometimes assumed all SO₂ transported into the upper cloud is oxidized to sulfuric acid. However, this may not be the case if the oxygen abundance in the upper cloud is sufficiently low, which is what is implied by the observational limits on O₂, assuming the observational limits are representative of global average conditions. Coupling between sulfur and chlorine chemistry may be important for understanding how the disproportionation of sulfur between sulfuric acid and polysulfur occurs, Section 6.3.

6. Coupled sulfur and chlorine chemistry

Reactions that couple sulfur and chlorine chemistry may play important roles in all three of the primary chemical cycles in Venus, atmosphere but have received comparatively less attention in photochemical models to date.

6.1. Coupled CO and SO₂ oxidation

Scheme F (Yung and DeMore, 1982) links the CO₂ and sulfur oxidation cycles via Reaction F7 and efficiently breaks the O–O bond in O₂, which is an important difference from Schemes A, B, and C. Scheme F likely requires vertical transport of SO because photodissociation of CO₂ occurs predominantly above 75 km altitude while photodissociation of SO₂ occurs predominately below 70 km altitude. Vertical transport of significant amounts of O₂ would likely require violating the observational upper limits on its abundance and the lifetime of ClO should be short.

6.2. Coupled Cl and SO₂ chemistry

Scheme G (DeMore et al., 1985) produces sulfuryl chloride, SO₂Cl₂, which could be a significant reservoir for chlorine although there have been arguments against this (Pollack et al., 1993). If a different loss pathway for ClSO₂,

Table 2
Reactions involving S_mCl_n and S_x

	Reaction	Rate coefficient ^a	Ref.
72	$SO + hv(\lambda < 232 \text{ nm}) \rightarrow S + O$	$J_{72} = 7.2 \times 10^{-4}$	b
74	$SO_2 + hv(\lambda < 210 \text{ nm}) \rightarrow S + O_2$	$J_{74} = 1.1 \times 10^{-6}$	c
79	$S_2 + hv(\lambda < 280 \text{ nm}) \rightarrow 2S$	$J_{79} = 1.2 \times 10^{-2}$	d
88	$SCl + hv(\lambda < 500 \text{ nm}) \rightarrow S + Cl$	$J_{88} = 1.1 \times 10^{-1}$	e
89	$SCl_2 + hv(\lambda < 460 \text{ nm}) \rightarrow SCl + Cl$	$J_{89} = 9.0 \times 10^{-3}$	f
91	$S_2Cl + hv(\lambda < 485 \text{ nm}) \rightarrow S_2 + Cl$	$J_{91} = 2.8 \times 10^{-1}$	e
151	$S + O_2 \rightarrow SO + O$	$k_{151} = 2.3 \times 10^{-12}$	g
167	$2SO \rightarrow SO_2 + S$	$k_{167} = 1 \times 10^{-12} e^{-1700/T}$	h
196	$ClSO_2 + SCl \rightarrow SO_2 + SCl_2$	$k_{196} = 5 \times 10^{-12}$	e
217	$2S + M \rightarrow S_2 + M$	$k_{217} k_0 = 1.18 \times 10^{-29}$ $k_\infty = 1 \times 10^{-10}$	i e
218	$S + S_2 + M \rightarrow S_3 + M$	$k_{218} k_0 = 1 \times 10^{-30}$ $k_\infty = 3 \times 10^{-11}$	e e
219	$2S_2 + M \rightarrow S_4 + M$	$k_{219} k_0 = 2.2 \times 10^{-29}$ $k_\infty = 1 \times 10^{-10}$	i j
226	$S_2 + S_4 + M \rightarrow S_6 + M$	$k_{226} k_0 = 1 \times 10^{-30}$ $k_\infty = 3 \times 10^{-11}$	e e
228	$2S_4 + M \rightarrow S_8 + M$	$k_{228} k_0 = 1 \times 10^{-30}$ $k_\infty = 3 \times 10^{-11}$	e e
240	$O + S_2 \rightarrow SO + S$	$k_{240} = 2 \times 10^{-11}$	k
242	$O + S_4 \rightarrow SO + S_3$	$k_{242} = 2 \times 10^{-11}$	e
262	$S + OCS \rightarrow S_2 + CO$	$k_{262} = 4 \times 10^{-12} e^{-1830/T}$	l
266	$S + Cl_2 \rightarrow SCl + Cl$	$k_{266} = 2.8 \times 10^{-11} e^{-290/T}$	m
267	$Cl + S_4 \rightarrow S_2Cl + S_2$	$k_{267} = 2 \times 10^{-12}$	e
268	$O + SCl \rightarrow SO + Cl$	$k_{268} = 1.2 \times 10^{-10}$	n
270	$Cl + SCl + M \rightarrow SCl_2 + M$	$k_{270} k_0 = 1 \times 10^{-30}$ $k_\infty = 5 \times 10^{-11}$	o e
271	$SCl + O_2 \rightarrow SO + ClO$	$k_{271} = 2 \times 10^{-15}$	p
272	$2SCl \rightarrow S_2 + Cl_2$	$k_{272} = 6 \times 10^{-12}$	q
290	$SO + Cl + M \rightarrow OSCl + M$	$k_{290} = 3 \times 10^{-33} \left(\frac{T}{300}\right)^{-5}$	e
292	$OSCl + Cl \rightarrow Cl_2 + SO$	$k_{292} = 2.3 \times 10^{-11}$	e
293	$SO + OSCl \rightarrow SO_2 + SCl$	$k_{293} = 6 \times 10^{-13}$	r
336	$SCl + S \rightarrow S_2 + Cl$	$k_{336} = 1 \times 10^{-11}$	s
337	$SCl + Cl_2 \rightarrow SCl_2 + Cl$	$k_{337} = 7 \times 10^{-14}$	t
339	$2SCl \rightarrow S_2Cl + Cl$	$k_{339} = 5.4 \times 10^{-11}$	q
344	$S_2Cl + Cl \rightarrow Cl_2 + S_2$	$k_{344} = 1 \times 10^{-11}$	s

^aThe units for mean photodissociation rates (J) and two-body and three-body reaction rates (k) are s^{-1} , $cm^3 s^{-1}$, and $cm^6 s^{-1}$, respectively. The numerical values for photodissociation refer to 70 km, mid-latitude.

^bData drawn from Colin (1969), Phillips (1981), Nee and Lee (1986), Manatt and Lane (1993), Phillips, personal communication (1992), and Manatt, personal communication (1993).

^cData drawn from Manatt and Lane (1993), Martinez and Joens (1992), Felder et al. (1988), Kawasaki and Sato (1987), and Ebata et al. (1988).

^dEstimated based on Oommen (1970), Watanabe et al. (1953), and Okabe (1978).

^eEstimated. See Mills (1998).

^fEstimated based on Colton and Rabalais (1974), Tiemann et al. (1989), Howe et al. (1995), and Samuel (1946).

^gSander et al. (2002).

^hMartinez and Herron (1983).

ⁱNicholas et al. (1979).

^jFowles et al. (1967).

^kSingleton and Cvetanovic (1988).

^lData drawn from Mallard et al. (1994).

^mBaulch et al. (1981).

ⁿMurrells (1988b).

^oEstimated based on Eibling and Kaufman (1983) and Murrells (1988a).

^p $0.1 \times$ upper limit from Murrells (1988b).

^qBased on Murrells (1988a).

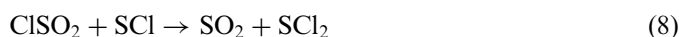
^rEstimated based on Donovan et al. (1969).

^sEstimated based on Murrells (1988a).

^tMurrells (1988a).

Reaction A.17, is important, then Scheme H (DeMore et al., 1985) may provide a means for increasing the rate of production of H₂SO₄. Scheme H may contribute significantly to the production of H₂SO₄ if the rate coefficient for Reaction A.17 is larger than about $2 \times 10^{-32} \text{ cm}^6 \text{ s}^{-1}$. This work has not been developed further as neither Reaction A.16 nor Reaction A.17 was included in the Table 1 models.

Reaction A.15, with loss of ClSO₂ via reactions,



was included in the Table 1 models and contributes to increasing the SO₂ scale height near 70 km altitude from ~2.5 km (Yung and DeMore, 1982) to ~3.0–3.5 km. Both scale heights are within the 2–4 km observational constraint (Na et al., 1994).

6.3. Chlorosulfane chemistry

Chlorosulfanes, S_mCl_n, have received very little attention but are likely to form in the upper cloud layer when the oxygen abundance is sufficiently small and the chlorine abundance is sufficiently large, as defined below. Table 2 lists the most important reactions involving chlorosulfanes and polysulfur in the Table 1 models (Mills, 1998).

The most important chlorosulfane pathways are shown in Figs. 2 and 3 for the +2σ and nominal CICO models, respectively.

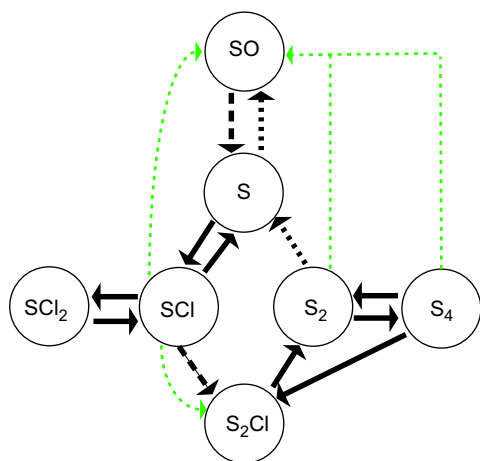


Fig. 2. Reactive pathways for production of polysulfur via chlorosulfanes in the +2σ CICO thermal stability model. (See notes for Table 1.) The solid black arrows indicate a pathway is important for both the production of the product and the loss of the reactant. The long-dashed black arrows indicate a pathway is important for the production of the product but not important for the loss of the reactant. The dotted black arrows indicate a pathway is important for the loss of the reactant but not important for the production of the product. A pathway was considered “important” if it contributes at least 10% of the total loss of these species. The pathways shown as green dotted arrows (for loss of S₂ to SO, S₄ to SO, SCl to SO, and SCl to S₂Cl) contribute 5–10% of the total loss of these species.

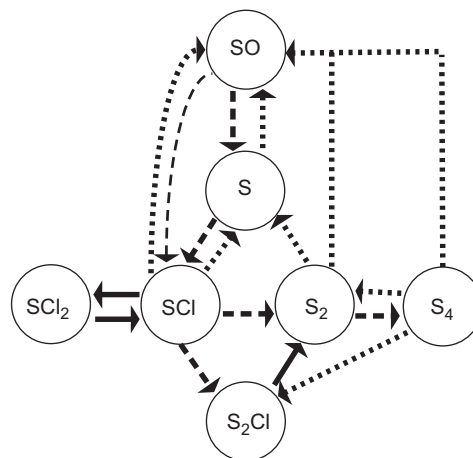


Fig. 3. Same as Fig. 2 for the nominal CICO thermal stability model. (See notes for Table 1.)

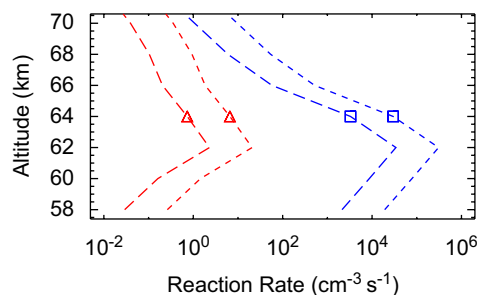


Fig. 4. Reaction rates for SCl loss pathways that lead to production of S₂ in the +2σ (blue with squares) and nominal (red with triangles) CICO thermal stability models. (See notes for Table 1.) Short dashed lines are for Reaction 339. Long dashed lines are for Reaction 272.

respectively. In both models, the primary path for production of S₂ is via SCl and S₂Cl. Almost all of the S₂Cl that is formed is lost via Reactions 91 and 344, so the net production of S₂ (excluding that from reactions destroying S_x where x > 2) is approximately the sum of the rates for Reactions 272 and 339. Production of S₂ occurs predominately at 59–65 km altitude, Fig. 4, and, as expected, the production rate for S₂ is markedly smaller in the nominal CICO thermal stability model.

There are three primary points at which the balance between production of S₄ and SO_x from S are determined, Figs. 2 and 3. The first is Reaction 151 versus Reaction 266. The second is Reactions 268 and 271 versus Reactions 272 and 339. The third is Reaction 240 versus Reaction 219. Assuming photochemical steady state, the balance between production of S_mCl_n (or S_x) and SO at each of these three primary branching points can be described by

$$\frac{\text{SCl production from S}}{\text{SO production from S}} = \frac{k_{266}[\text{Cl}_2]}{k_{151}[\text{O}_2]}, \quad (9)$$

$$\frac{\text{S}_2\text{Cl and S}_2 \text{ production from SCl}}{\text{SO production from SCl}} = \frac{(k_{272} + k_{339})[\text{SCl}]}{(k_{268}[\text{O}] + k_{271}[\text{O}_2])}, \quad (10)$$

$$\frac{S_4 \text{ production from } S_2}{SO \text{ production from } S_2} = \frac{k_{219}[S_2][M]}{k_{240}[O]}, \quad (11)$$

where the concentrations of S, SCl, and S₂ at 59–65 km altitude (in steady state) are given approximately by

$$[S] \approx \frac{J_{72}[SO] + J_{88}[SCl]}{k_{151}[O_2] + k_{266}[Cl_2]}, \quad (12)$$

$$[SCl] \approx \frac{k_{266}[S][Cl_2]}{J_{88} + k_{268}[O]} + \frac{k_{293}k_{290}[SO]^2[M]}{(J_{88} + k_{268}[O])(k_{292})}, \quad (13)$$

$$[S_2] \approx \frac{k_{339}[SCl]^2}{J_{79} + k_{240}[O]}, \quad (14)$$

respectively.

Based on these (approximate) equations, the branching ratios for production of polysulfur and SO are determined by the concentrations of O, O₂, SO, and Cl₂, Fig. 5. The most significant differences between the +2σ and the nominal CICO thermal stability models in Fig. 5 are the concentrations of SO and O₂, with the latter difference larger by two orders of magnitude than the former. Consequently, the differences in production rates for S₂ (and, thus, for polysulfur) for these two models, Fig. 4, appear to be largely controlled by the O₂ concentrations. Fig. 6 shows the change in branching ratios for loss of S, Fig. 7 shows the change in branching ratios for loss of SCl, and Fig. 8 shows the change in branching ratios for loss of

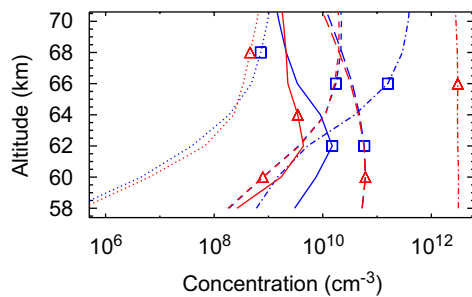


Fig. 5. Concentrations of O, O₂, Cl, Cl₂, and SO in the +2σ (blue with squares) and nominal (red with triangles) CICO thermal stability models. (See notes for Table 1.) Dotted lines are [O], dash-dot lines are [O₂], short-dash lines are [Cl], long-dash lines are [Cl₂], and solid lines are [SO].

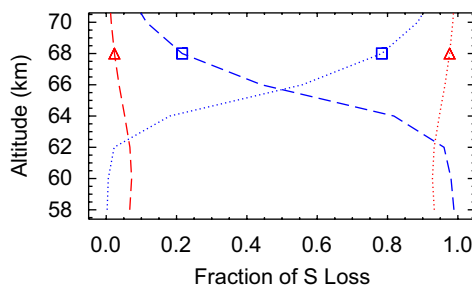


Fig. 6. Oxidation and reduction loss paths for S in the +2σ (blue with squares) and nominal (red with triangles) CICO thermal stability models. (See notes for Table 1.) Dotted lines are Reaction 151; dashed lines are Reaction 266.

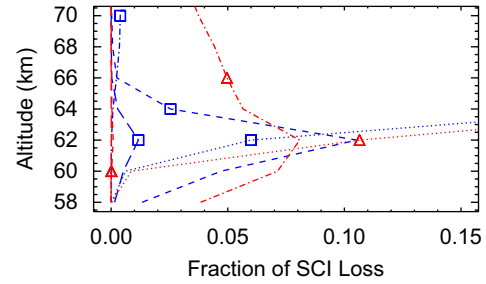


Fig. 7. Oxidation and reduction loss paths for SCl in the +2σ (blue with squares) and nominal (red with triangles) CICO thermal stability models. (See notes for Table 1.) Dotted lines are Reaction 268; dash-dot lines are Reaction 271; short-dash lines are Reaction 339; long-dash lines are Reaction 272. The fraction of SCl lost via Reaction 268 increases monotonically with altitude to 0.50 (nominal model) and 0.61 (+2σ model) at 70 km altitude.

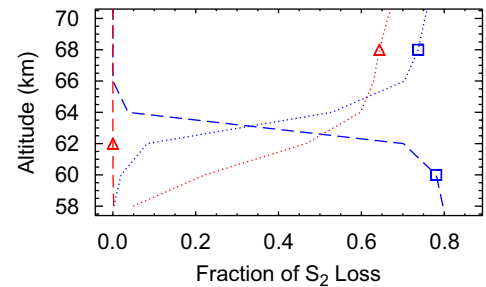


Fig. 8. Oxidation and reduction loss paths for S₂ in the +2σ (blue with squares) and nominal (red with triangles) CICO thermal stability models. (See notes for Table 1.) Dotted lines are Reaction 240; dashed lines are Reaction 219.

S₂. The fraction of the loss not shown in these figures is recycled to earlier stages in the polysulfur production process, Figs. 2 and 3.

The rate coefficients in Eq. (9) have been measured and critically assessed, so the uncertainties in this ratio are probably the best constrained among Eqs. (9)–(11). For Eq. (10), the individual rate coefficients in the numerator, k_{272} and k_{339} , have not been determined but their sum has been measured (Murrells, 1988a). In the denominator, k_{268} has been measured but only an upper limit exists for k_{271} . Even if k_{271} were as large as the upper limit, $2 \times 10^{-14} \text{ cm}^3 \text{ s}^{-1}$ (Murrells, 1988b), Eq. (10) would decrease by less than a factor of two in the +2σ model, which is probably the closest model to the real Venus atmosphere at least for O₂ concentrations. The rate coefficients in Eq. (11) have also been measured but their temperature dependences are also not known. The uncertainties in Eqs. (9)–(11) due to uncertainties in the rate coefficients are 50% at 250 K, at least 60% with unknown temperature dependence, and at least 300% at 298 K with unknown temperature dependence, respectively. The primary uncertainties regarding the efficiency of the proposed chlorosulfane mechanism for producing S₂, however, are likely to be whether there are important oxidation loss channels for S₂Cl and SCl₂, which were not included in the present

models. These modeling results and the branching ratio equations derived above together suggest that the chlorosulfane pathways in Fig. 2 are likely to be important if the O₂ abundance is as low as the observational limits imply, regardless of whether the low O₂ abundance results from fast CO oxidation or fast SO₂ oxidation. The predicted chlorosulfane abundances are small (<1 ppbv) so their identification via remote sensing may be difficult.

7. Conclusions

Progress has been made in the past 20 years in understanding the CO₂ cycle in Venus' atmosphere, but major questions remain unanswered. Oxidation of CO to CO₂ via chlorine catalytic reactions (Krasnopolsky and Parshev, 1981a–c, 1983; Yung and DeMore, 1981, 1982) has been verified in laboratory experiments (Pernice et al., 2004), but significant uncertainties remain in the rate coefficients for each step in this mechanism (Sander et al., 2002). Although the uncertainty on the thermal stability of ClCO is small by laboratory standards, model calculations are very sensitive to this parameter, so further laboratory study is required. Within the large uncertainty induced by uncertainty in the thermal stability of ClCO, it is possible to construct a model whose column O₂ abundance is roughly consistent with the observational upper limit. Two other proposed CO oxidation mechanisms—the aerosol mechanism which may be important below 70 km and the O₂(c) mechanism which may be important above 90 km—await laboratory confirmation. Advances in our understanding of excited state oxygen chemistry have enabled models to simulate the observed global average airglow in the 1.27 μm O₂(a¹Δ → X³Σ) band. Further progress is needed to address the larger question of simultaneously understanding the column O₂ abundance and the CO distribution. This question will require global observations of the abundances of ground-state O₂, O₂ airglow, and CO at 50–100 km.

Further laboratory experiments, observations, and numerical modeling are required to understand: (1) the mechanism(s) and rate(s) for production of H₂SO₄, (2) the interactions that may occur among sulfur, chlorine, and nitrogen radicals, and (3) the interactions between chemistry and dynamics. The first of these is a key point of disagreement between cloud and photochemical models that needs to be resolved. The solution may also improve the agreement between modeled O₂ abundances and the observational upper limits. The second provides key links among the primary chemical cycles, especially in the upper cloud layer, and likely provides important pathways for the production of H₂SO₄ and S_x. Both the first and second will require modeling and observational data over the depth of the cloud layers. Observations of SO, SO₂, and OCS at 50–75 km altitude should help resolve these questions, particularly if the scale height of SO₂ can be constrained to within 0.5 km. The third will require development of a

multidimensional chemical transport model based on global observations of winds, temperatures, and CO abundances.

Venus Express data will provide a more comprehensive and detailed view than exists today for CO, SO, SO₂, OCS, O₂ airglow, winds, and temperatures. Detection of ClCO, ClC(O)OO, or COCl₂ would be a major confirmation of the ClC(O)OO mechanism for CO oxidation, while an anti-correlation between oxygen green line emission and 1.27 μm airglow would lend support to the O₂(c) mechanism for CO oxidation. These data and the supporting laboratory experiments, earth-based observations, and numerical modeling should produce significant advances in our understanding of the rich chemistry that appears to occur within Venus' atmosphere.

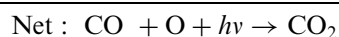
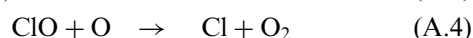
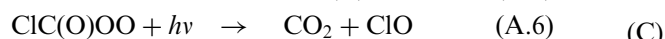
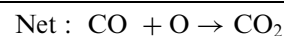
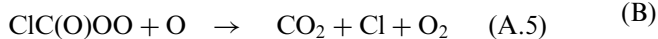
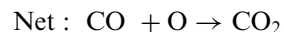
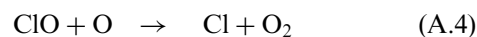
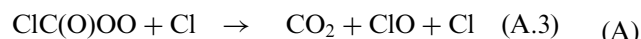
Acknowledgements

Partial funding for this research was provided by the NASA Planetary Astronomy and Atmospheres programs and the Australian Research Council. Part of this work was performed at the Jet Propulsion Laboratory, California Institute of Technology, under contract to the National Aeronautics and Space Administration. Helpful comments from B. Burns, S. Cavanagh, S. Gibson, T. Slanger, and F. Taylor are gratefully acknowledged. Helpful reviews from V. Krasnopolsky and an anonymous reviewer are gratefully acknowledged.

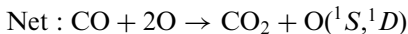
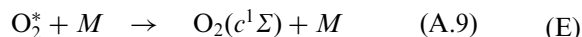
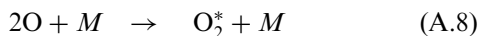
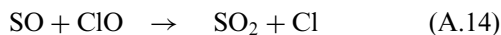
Appendix A. Chemical schemes from previous studies referenced in text

The chemical schemes referenced in the main text from previous studies are detailed below.

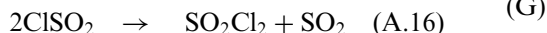
A.1. CO Oxidation via ClC(O)OO



A.2. CO oxidation via heterogeneous processes

A.3. CO oxidation via reaction with O₂(c¹Σ)A.4. Coupled CO and SO₂ oxidation

A.5. Sulfuryl chloride production

A.6. SO₂ oxidation via ClSO₄

References

- Allen, M., Yung, Y.L., Waters, J.W., 1981. Vertical transport and photochemistry in the terrestrial mesosphere and lower thermosphere. *J. Geophys. Res.* 86, 3617–3627.
- Anderson, S.M., Mauersberger, K., 1992. Laser measurements of ozone absorption cross sections in the Chappuis Band. *Geophys. Res. Lett.* 19, 933–936.
- Atreya, S.K., Blamont, J.E., 1990. Stability of the Martian atmosphere: Possible role of heterogeneous chemistry. *Geophys. Res. Lett.* 17, 287–290.
- Baulch, D.L., Duxbury, J., Grant, S.J., Montague, D.C., 1981. Evaluated Kinetic Data for High Temperature Reactions, Volume 4: Homo-

- geneous Gas Phase Reactions of halogen- and cyanide-containing species. American Chemical Society.
- Bednarek, G.P.W.R., Wildt, J., Fink, E.H., 1994. The yield of O₂(b¹Σ_g⁺, v = 0) produced by quenching of O₂(A³Σ_u⁺, v = 8) by O₂. *Chem. Phys.* 185, 251–261.
- Bezard, B., deBergh, C., Crisp, D., Maillard, J.-P., 1990. The deep atmosphere of Venus revealed by high-resolution nightside spectra. *Nature* 345, 508–511.
- Burkholder, J.B., Talukdar, R.K., 1994. Temperature dependence of the ozone absorption spectrum over the wavelength range 410 to 760 nm. *Geophys. Res. Lett.* 21, 581–584.
- Choi, W., Leu, M.-T., 1997. Kinetics of the heterogeneous reaction CO + O → CO₂ on inorganic oxide and water ice surfaces: implications for the Martian atmosphere. *Geophys. Res. Lett.* 24, 2957–2960.
- Clancy, R., Muhleman, D., 1991. Long-term (1979–1990) changes in the thermal, dynamical, and compositional structure of the Venus mesosphere as inferred from microwave spectral line observations of ¹²CO, ¹³CO, and C¹⁸O. *Icarus* 89, 129–146.
- Clancy, R., Sandor, B., Moriarty-Schieven, G., 2003. Observational definition of the Venus mesopause: vertical structure, diurnal variation, and temporal instability. *Icarus* 161, 1–16.
- Colin, R., 1969. Spectrum of SO: Analysis of the B³Σ⁻ – X³Σ⁻ and A³Π – X³Σ⁻ band systems. *Can. J. Phys.* 47, 979–994.
- Colton, R.J., Rabalais, J.W., 1974. Photoelectron and electronic absorption spectra of SCl₂, S₂Cl₂, S₂Br₂, and (CH₃)₂S₂. *J. Electr. Spectr. Rel. Phenom.* 3, 345–357.
- Connes, P., Connes, J., Kaplan, L., Benedict, W., 1967. Traces of HCl and HF in the atmosphere of Venus. *Astrophys. J.* 147, 1230–1237.
- Connes, P., Connes, J., Kaplan, L.D., Benedict, W.S., 1968. Carbon monoxide in the Venus atmosphere. *Astrophys. J.* 152, 731–743.
- Connes, P., Connes, J., Noxon, F., Traub, W., Carlton, N., 1979. O₂(¹Δ) emission in the day & night airglow of Venus. *Astrophys. J.* 233, L29–L32.
- Crisp, D., 1986. Radiative forcing of the Venus mesosphere I: Solar fluxes and heating rates. *Icarus* 67, 484–514.
- Crisp, D., Meadows, V.S., Bezard, B., de Bergh, C., Maillard, J.-P., Mills, F.P., 1996. Ground-based near-infrared observations of the Venus night side: near-infrared O₂(¹Δ) airglow from the upper atmosphere. *J. Geophys. Res.* 101, 4577–4593.
- DeMore, W., Leu, M.-T., Smith, R., Yung, Y., 1985. Laboratory studies on the reactions between chlorine, sulfur dioxide, and oxygen: Implications for the Venus stratosphere. *Icarus* 63, 347–353.
- DeMore, W.B., Sander, S.P., Golden, D.M., Hampson, R.F., Kurylo, M.J., Howard, C.J., Ravishankara, A.R., Kolb, C.E., Molina, M.J., 1997. Chemical kinetics and photochemical data for use in stratospheric modeling: Evaluation number 12. JPL Publication 97-4, Jet Propulsion Laboratory, Pasadena, CA.
- Donovan, R.J., Husain, D., Jackson, P.T., 1969. Spectroscopic and kinetic studies of the SO radical and the photolysis of thionyl chloride. *Trans. Faraday Soc.* 65, 2930–2940.
- Ebata, T., Nakazawa, O., Ito, M., 1988. Rovibrational dependences of the predissociation in the C¹B₂ state of SO₂. *Chem. Phys. Lett.* 143, 31–37.
- Eibling, R.E., Kaufman, M., 1983. Kinetics studies relevant to possible coupling between the stratospheric chlorine and sulfur cycles. *Atmos. Environ.* 17, 429–431.
- Eposito, L.W., Bertaux, J.-L., Krasnopolsky, V., Moroz, V.I., Zasova, L.V., 1997. Chemistry of lower atmosphere and clouds. In: Bougher, S.W., Hunten, D.M., Phillips, R.J. (Eds.), *Venus II*. University of Arizona Press, Tucson, AZ, pp. 415–458.
- Eposito, L.W., Copley, M., Eckert, R., Gates, L., Stewart, A.I.F., Worden, H., 1988. Sulfur dioxide at the Venus cloud tops, 1978–1986. *J. Geophys. Res.* 93, 5267–5276.
- Felder, P., Effenhauser, C.S., Haas, B.M., Huber, J.R., 1988. Photodissociation of sulfur dioxide at 193 nm. *Chem. Phys. Lett.* 148, 417–422.
- Fink, E.H., Setzer, K.D., Wildt, J., 1991. Collision-induced emission of O₂(b¹Σ_g⁺ → a¹Δ_g) in the gas phase. *Int. J. Quant. Chem.* 39, 287–298.

- Fowles, P., deSorgo, J., Yarwood, A.J., Strausz, O.P., Gunning, H.E., 1967. The reactions of sulfur atoms IX. The flash photolysis of carbonyl sulfide and the reactions of (S^1D) atoms with hydrogen and methane. *J. Amer. Chem. Soc.* 89, 1352–1362.
- Freeman, D.E., Yoshino, K., Esmond, J.R., Parkinson, W.H., 1984a. High resolution absorption cross-section measurements of ozone at 195 k in the wavelength region 240–350 nm. *Planet. Space Sci.* 32, 239–248.
- Freeman, D.E., Yoshino, K., Esmond, J.R., Parkinson, W.H., 1984b. High resolution absorption cross-section measurements of SO_2 at 213 K in the wavelength region 172–240 nm. *Planet. Space Sci.* 32, 239–248.
- Griggs, M., 1968. Absorption coefficients of ozone in the ultraviolet and visible regions. *J. Chem. Phys.* 49, 857–859.
- Gurwell, M., Muhleman, D., Shah, K., Berge, G., Rudy, D., Grossman, A., 1995. Observations of the CO bulge on Venus and implications for mesospheric winds. *Icarus* 115, 141–158.
- Hearn, C.H., Joens, J.A., 1991. The near UV absorption spectrum of CS_2 and SO_2 at 300 K. *J. Quant. Spectrosc. Radiat. Transfer* 45, 69–75.
- Howe, J.D., Ashford, M.N.R., Morgan, R.A., Western, C.M., Buma, W.J., Milan, J.B., de Lange, C.A., 1995. Observation of the SCl radical by resonance-enhanced multiphoton ionisation spectroscopy. *J. Chem. Soc. Faraday Trans.* 91, 773–780.
- Huestis, D.L., 2002. Current laboratory experiments for planetary aeronomy. In: Mendillo, M., Nagy, A., Waite, J.H. (Eds.), *Atmospheres in the Solar System: Comparative Aeronomy*. Geophysical Monograph, vol. 130. American Geophysical Union, Washington, DC, pp. 245–258.
- Ignatiev, N.I., Moroz, V.I., Moshkin, B.E., Ekonomov, A.P., Gnedykh, V.I., Grigoriev, A.V., Khatuntsev, I.V., 1997. Water vapour in the lower atmosphere of Venus: a new analysis of optical spectra measured by entry probes. *Planet. Space Sci.* 45, 427–438.
- Kawasaki, M., Sato, H., 1987. Photodissociation of molecular beams of SO_2 at 193 nm. *Chem. Phys. Lett.* 139, 585–588.
- Knutsen, K., Dyer, M.J., Copeland, R.A., 1994. Laser double-resonance study of the collisional removal of $O_2(A^3\Sigma_u^+, v = 6, 7, 9)$ with O_2 , N_2 , CO_2 , Ar and He. *J. Chem. Phys.* 101, 7415–7422.
- Krasnopolsky, V.A., 1983. Venus spectroscopy in the 3000–8000 Å region by Veneras 9 and 10. In: Hunten, D.M., Colin, L., Donohue, T.M., Moroz, V.I. (Eds.), *Venus*. University of Arizona Press, Tucson, AZ, pp. 459–483.
- Krasnopolsky, V.A., 1986. *Photochemistry of the Atmospheres of Mars and Venus*. Springer, New York.
- Krasnopolsky, V.A., 2006a. Chemical composition of Venus atmosphere and clouds: Some unsolved problems. *Planet. Space Sci.* 54, 1352–1359.
- Krasnopolsky, V.A., 2006b. A sensitive search for nitric oxide in the lower atmosphere of Venus and Mars: Detection on Venus and upper limit for Mars. *Icarus* 182, 80–91.
- Krasnopolsky, V.A., Krysko, A.A., Rogachev, V.N., Parshev, V.A., 1976. Spectroscopy of the night-sky luminescence of Venus from the interplanetary spacecraft Venera 9 and Venera 10. *Cosmic Res.* 14, 687–692 (translated from *Kosmich. Issled.*, 14, 789–795, 1976).
- Krasnopolsky, V.A., Parshev, V.A., 1981a. Chemical composition of the atmosphere of Venus. *Nature* 292, 610–613.
- Krasnopolsky, V.A., Parshev, V.A., 1981b. Photochemistry of the atmosphere of Venus at altitudes greater than 50 km II. Calculations. *Cosmic Res.* 19, 176–189 (translated from *Kosmich. Issled.* 19, 261–278, 1981).
- Krasnopolsky, V.A., Parshev, V.A., 1981c. Photochemistry of Venus' atmosphere at altitudes over 50 km I. Initial calculation data. *Cosmic Res.* 19, 61–74 (translated from *Kosmich. Issled.* 19, 87–104, 1981).
- Krasnopolsky, V.A., Parshev, V.A., 1983. Photochemistry of the Venus atmosphere. In: Hunten, D.M., Colin, L., Donohue, T.M., Moroz, V.I. (Eds.), *Venus*. University of Arizona Press, Tucson, AZ, pp. 431–458.
- Krasnopolsky, V.A., Pollack, J.B., 1994. H_2O – H_2SO_4 system in Venus' clouds and OCS, CO, and H_2SO_4 profiles in Venus' troposphere. *Icarus* 109, 58–78.
- Lane, W.A., Opstbaum, R., 1983. High altitude Venus haze from Pioneer Venus limb scans. *Icarus* 54, 48–58.
- Lawrence, G.M., Barth, C.A., Argabright, V., 1977. Excitation of the Venus night airglow. *Science* 195, 573–574.
- Lellouch, E., Goldstein, J.J., Rosenqvist, J., Bougher, S.W., Paubert, G., 1994. Global circulation, thermal structure, and carbon monoxide distribution in Venus' mesosphere in 1991. *Icarus* 110, 315–339.
- Leroy, B., Rigaud, P., Jourdain, J.L., LeBras, G., 1983. Spectres d'absorption dans le proche ultraviolet de CS_2 et SO_2 entre 200 et 300 K. *The Moon and the Planets* 29, 177–183.
- Lewis, B.R., Carver, J.H., 1983. Temperature dependence of the carbon dioxide photoabsorption cross section between 1200 and 1970 Å. *J. Quant. Spectrosc. Radiat. Transfer* 30, 297–309.
- Maiorov, B.S., Ignat'ev, N.I., Moroz, V.I., Zasova, L.V., Moshkin, B.E., Khatuntsev, I.V., Ekonomov, A.P., 2005. A new analysis of the spectra obtained by the *Venera* missions in the Venusian atmosphere. I. the analysis of the data received from the *Venera-11* probe at altitudes below 37 km in the 0.44–0.66 μm wavelength range. *Solar Syst. Res.* 39, 267–282.
- Mallard, W.G., Westley, F., Herron, J.T., Hampson, R.F., 1994. NIST Chemical Kinetics Database version 6.0. National Institute of Standards and Technology Standard Reference Data, Gaithersburg, MD.
- Manatt, S.L., Lane, A.L., 1993. A compilation of the absorption cross-sections of SO_2 from 106 to 403 nm. *J. Quant. Spectrosc. Radiat. Transfer* 50, 267–276.
- Martinez, R., Herron, J., 1983. Methyl thiirane: Kinetic gas-phase titration of sulfur atoms in S_xO_y systems. *Int. J. Chem. Kin.* 15, 1127.
- Martinez, R.D., Joens, J.A., 1992. SO_2 absorption cross-section measurements from 197 nm to 240 nm. *Geophys. Res. Lett.* 19, 277–279.
- McGee, T.J., J.R., Burris, J., 1987. SO_2 absorption cross sections in the near UV. *J. Quant. Spectrosc. Radiat. Transfer* 37, 165–182.
- Mills, F.P., 1998. I. observations and photochemical modeling of the Venus middle atmosphere. II. thermal infrared spectroscopy of Europa and Callisto. Ph.D. dissertation, California Institute of Technology, Pasadena, CA, 366pp.
- Mills, F.P., 1999a. A spectroscopic search for molecular oxygen in the Venus middle atmosphere. *J. Geophys. Res.* 104, 30757–30764.
- Mills, F.P., 1999b. Water vapour in the Venus middle atmosphere. *Advances in Space Research* 23, 1573–1576.
- Mills, C., Phillips, L., 1993. Photo-oxidation of CO in a sulphuric acid aerosol. *J. Photochem. Photobiol. A: Chem.* 74, 7–9.
- Mills, C., Phillips, L., 1996. Quantum yields of CO_2 and SO_2 formation from 193 nm photooxidation of CO. *J. Photochem. Photobiol. A: Chem.* 93, 83–87.
- Mills, F.P., Esposito, L.W., Yung, Y.L., 2007. Atmospheric composition, chemistry, and clouds. In: Esposito, L.W., Stofan, E., Cravens, T. (Eds.), *Exploring Venus as a Terrestrial Planet*. American Geophysical Union, Washington, DC under review.
- Mills, F.P., Sundaram, M., Slinger, T.G., Allen, M., Yung, Y.L., 2006. Oxygen chemistry in the Venus middle atmosphere. In: Ip, W.-H., Bhardwaj, A. (Eds.), *Advances in Geosciences Volume 3: Planetary Science (PS)*. World Scientific Publishing Co., Singapore, pp. 109–117.
- Molina, L.T., Lamb, J.J., Molina, M.J., 1981. Temperature dependent UV absorption cross sections for carbonyl sulfide. *Geophys. Res. Lett.* 8, 1008–1011.
- Molina, L.T., Molina, J.J., 1986. Absolute absorption cross sections of ozone in the 185- to 350-nm wavelength range. *J. Geophys. Res.* 91, 14501–14508.
- Murrells, T.P., 1988a. Elementary reactions of the SCl radical part 1.—rate constants and mechanisms of the reactions $Cl + C_2HS \rightarrow SCl + C_2H_4$, $SCl + SCl \rightarrow$ products and $SCl + Cl_2 \rightarrow SCl_2 + Cl$. *J. Chem. Soc. Faraday Trans. II* 84, 67–83.

- Murrells, T.P., 1988b. Elementary reactions of the SCl radical part 2.— rate constants and mechanisms of the reactions of SCl with NO₂, NO, O₂, O(³P), and N(⁴S). *J. Chem. Soc. Faraday Trans. II* 84, 85–94.
- Na, C.Y., Esposito, L.W., McClintock, W.E., Barth, C.A., 1994. Sulfur dioxide in the atmosphere of Venus. *Icarus* 112, 389–395.
- Nair, H., Allen, M., Anbar, A.D., Yung, Y.L., Clancy, R.T., 1994. A photochemical model of the Martian atmosphere. *Icarus* 111, 124–150.
- Nee, J.B., Lee, L.C., 1986. Vacuum ultraviolet photoabsorption study of SO. *J. Chem. Phys.* 84, 5303–5307.
- Nicholas, J.E., Amodio, C.A., Baker, M.J., 1979. Kinetics and mechanism of the decomposition of H₂S, CH₃SH and (CH₃)₂S in a radio-frequency pulse discharge. *J. Chem. Soc. Faraday Trans. I* 75, 1868–1875.
- Nicovich, J., Kreutter, K., Wine, P., 1990. Kinetics and thermochemistry of ClCO formation from the Cl + CO association reaction. *J. Chem. Phys.* 92, 3539–3544.
- Okabe, H., 1978. *Photochemistry of Small Molecules*. Wiley, New York.
- Oommen, 1970. Spectra and reactions of elemental sulfur. Ph.D. thesis, University of Washington, Seattle, WA.
- Oyama, V.I., Carle, G.C., Woeller, F., Pollack, J.B., Reynolds, R.T., Craig, R.A., 1980. Pioneer Venus gas chromatography of the lower atmosphere of Venus. *J. Geophys. Res.* 85, 7891–7902.
- Pernice, H., Garcia, P., Willner, H., Francisco, J.S., Mills, F.P., Allen, M., Yung, Y.L., 2004. Laboratory evidence for a key intermediate in the Venus atmosphere: Peroxychloroformyl radical. *Proc. Natl. Acad. Sci.* 101, 14007–14010.
- Phillips, L., 1981. Absolute absorption cross sections for SO between 190 and 235 nm. *J. Phys. Chem.* 85, 3994–4000.
- Pollack, J.B., Dalton, J.B., Grinspoon, D., Wattson, R.B., Freedman, R., Crisp, D., Allen, D.A., Bezdard, B., deBergh, C., Giver, L.P., Ma, Q., Tipping, R., 1993. Near-infrared light from Venus' nightside: a spectroscopic analysis. *Icarus* 103, 1–42.
- Porshnev, N.V., Mukhin, L.M., Gelman, B.G., Nenarokov, D.F., Rotin, V.A., Dyachkov, A.V., Bondarev, V.B., 1987. Gas chromatographic analysis of the products of thermal reactions of Venus cloud aerosols on the Vega-1 and -2 automated interplanetary probes. *Cosmic Res.* 25, 549–553 (translated from *Kosmich. Issled.* 25, 715–720, 1987).
- Prinn, R.G., 1978. Chemistry of the lower atmosphere prior to the Pioneer Venus mission. *Geophys. Res. Lett.* 5, 973–976.
- Rowland, G.A., Phillips, L.F., 2000. Cloud photochemistry and its effect on the composition of the upper atmosphere of Venus. *Geophysical Research Letters* 27, 3301–3304.
- Rowland, G.A., van Eldik, R., Phillips, L.F., 2002. Photochemistry of concentrated sulphuric acid in the presence of SO₂ and Fe(II), and implications for the cloud chemistry of Venus. *J. Photochem. Photobiol. A: Chemistry* 153, 1–10.
- Samuel, R., 1946. The dissociation spectra of covalent polyatomic molecules. *Rev. Modern Phys.* 18, 103–147.
- Sander, S.P., et al., 2002. Chemical kinetics and photochemical data for use in stratospheric modeling evaluation number 14. JPL Publication 02-25, Jet Propulsion Laboratory, Pasadena, CA, (<http://www.jpldataeval.jpl.nasa.gov/>).
- Seiff, A., 1983. Models of Venus's atmospheric structure. In: Hunten, D.M., Colin, L., Donohue, T.M., Moroz, V.I. (Eds.), *Venus*. University of Arizona Press, Tucson, AZ, pp. 1045–1048.
- Shemansky, D.E., 1972. CO₂ extinction coefficient 1700–3000 Angstrom. *J. Chem. Phys.* 56, 1582–1587.
- Singleton, D.L., Cvetanovic, R.J., 1988. Evaluated chemical kinetic data for the reactions of atomic oxygen (O³P) with sulfur containing compounds. *J. Phys. Chem. Ref. Data* 17, 1377–1437.
- Slanger, T.G., Copeland, R.A., 2003. Energetic oxygen in the upper atmosphere and the laboratory. *Chemical Reviews* 103, 4731–4765.
- Slanger, T.G., Huestis, D.L., Cosby, P.C., Chanover, N.J., Bida, T.A., 2006. The Venus nightglow: ground-based observations and chemical mechanisms. *Icarus* 182, 1–9.
- Sprague, K.E., Joens, J.A., 1995. SO₂ absorption cross-section measurements from 320 nm to 405 nm. *J. Quant. Spectrosc. Radiat. Transfer* 53, 349–352.
- Sundaram, M., Mills, F.P., Yung, Y.L., Allen, M., 2007. Heterogeneous oxidation of CO in the Venus middle atmosphere, in preparation.
- Suto, M., Day, R.L., Lee, L.C., 1982. Fluorescence yields from photodissociation of SO₂ at 1060–1330 Angstrom. *J. Phys. B: At. Mol. Phys.* 15, 4165–4174.
- Tanaka, Y., Inn, E.C.Y., Watanabe, K., 1953. Absorption coefficients of gases in the vacuum ultraviolet, part IV. ozone. *J. Chem. Phys.* 21, 1651–1653.
- Thevenet, A., Juillet, F., Teichner, S.J., 1974. Photointeraction on the surface of titanium dioxide between oxygen and carbon monoxide. *Japan J. Appl. Phys. Suppl.* 2 (Pt. 2), 529–532 (Proceedings of the Second International Conference on Solid Surfaces).
- Tiemann, E., Kanamori, H., Hirota, E., 1989. Infrared diode laser spectroscopy of SCl generated by the photolysis of S₂Cl₂ and SCl₂. *J. Molec. Spectrosc.* 137, 278–285.
- Traub, W.A., Carleton, N.P., 1974. Observation of O₂, H₂O, and HD in planetary atmospheres. In: Woszczyk, A., Iwaniszewska, C. (Eds.), *Exploration of the Planetary System*. Reidel, Dordrecht, The Netherlands, pp. 223–228.
- Trauger, J., Lunine, J., 1983. Spectroscopy of molecular oxygen in the atmospheres of Venus and Mars. *Icarus* 55, 272–281.
- von Zahn, U., Fricke, K.H., Hunten, D.M., Krankowsky, D., Mauersberger, K., Nier, A.O., 1980. The upper atmosphere of Venus during morning conditions. *J. Geophys. Res.* 85, 7829–7840.
- von Zahn, U., Kumar, S., Niemann, H., Prinn, R., 1983. Composition of the Venus atmosphere. In: Hunten, D.M., Colin, L., Donohue, T.M., Moroz, V.I. (Eds.), *Venus*. University of Arizona Press, Tucson, AZ, pp. 299–430.
- Watanabe, K., Inn, E.C.Y., Zelikoff, M., 1953. Absorption coefficients of oxygen in the vacuum ultraviolet. *J. Chem. Phys.* 21, 1026–1030.
- Wildt, J., Bednarek, G., Fink, E.H., 1988. Laser excitation of O₂(b¹Σ_g⁺, v = 0, 1, 2)-rates and channels of energy transfer and quenching. *Chem. Phys.* 122, 463–470.
- Wildt, J., Bednarek, G., Fink, E.H., Wayne, R.P., 1991. Laser excitation of the A³Σ_g⁺, A³A_u and c¹Σ_u⁻ states of molecular oxygen. *Chem. Phys.* 156, 497–508.
- Winick, J.R., Stewart, A.I., 1980. Photochemistry of SO₂ in Venus' upper cloud layers. *J. Geophys. Res.* 85, 7849–7860.
- Woo, R., Ishimaru, A., 1981. Eddy diffusion coefficient for the atmosphere of Venus from radio scintillation measurements. *Nature* 289, 383–384.
- Yoshino, K., Freeman, D.W., Esmond, J.R., Parkinson, W.H., 1988. Absolute absorption cross-section measurements of ozone in the wavelength region 238–335 nm and the temperature dependence. *Planet. Space Sci.* 36, 395–398.
- Yoshino, K., Esmond, J.R., Freeman, D.E., Parkinson, W.H., 1993. Measurements of absolute absorption cross sections of ozone in the 185- to 254-wavelength region and the temperature dependence. *J. Geophys. Res.* 98, 5205–5211.
- Young, L.D.G., 1972. High resolution spectrum of Venus—a review. *Icarus* 17, 632–658.
- Yung, Y.L., DeMore, W.B., 1981. Photochemical models for the stratosphere of Venus. In: *An International Conference on the Venus Environment*. NASA Ames Research Center, p. 26.
- Yung, Y.L., DeMore, W.B., 1982. Photochemistry of the stratosphere of Venus: Implications for atmospheric evolution. *Icarus* 51, 199–247.